AD-A056 843 SRI INTERNATIONAL MENLO PARK CA F/G 4/1
DETERMINATION OF NO2 PHOTOLYSIS PARAMETERS FOR STRATOSPHERIC MO--ETC(U).
JUN 78 J E DAVENPORT DOT-TSC-1204

UNCLASSIFIED FAA-EQ-78-05 NL

1 OF 1
ADA
056843

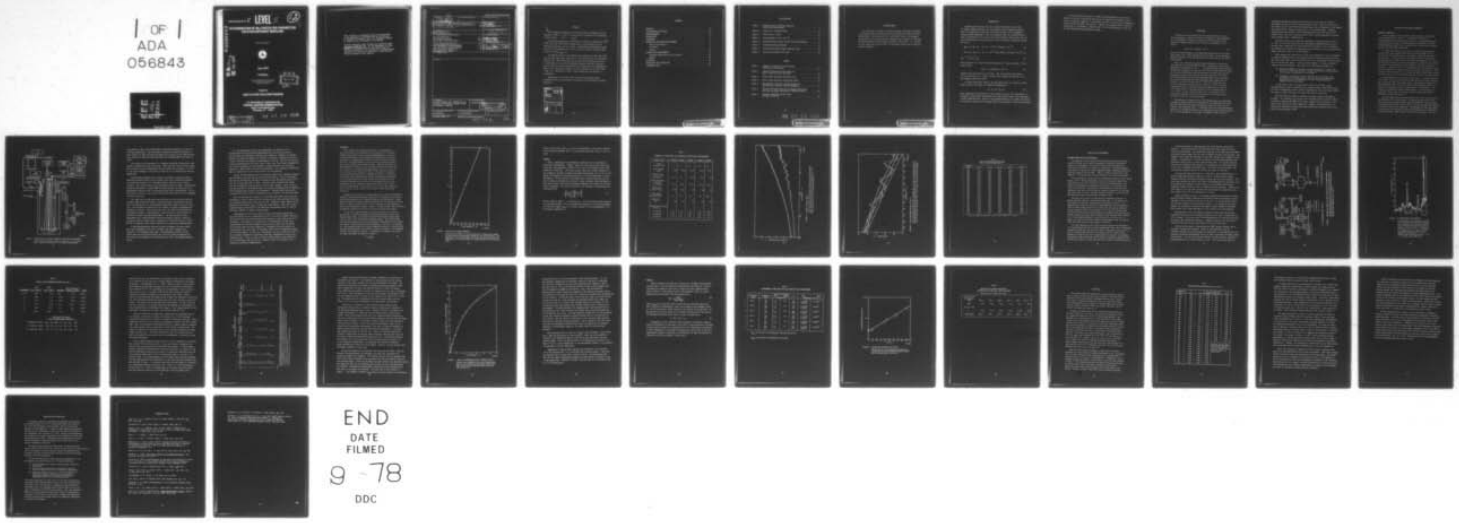

END
DATE
FILMED
9-78
DDC

Report No. FAA-EQ-78-05

LEVEL II

12

DETERMINATION OF NO_2 PHOTOLYSIS PARAMETERS FOR STRATOSPHERIC MODELING

John E. Davenport

June 1978

Final Report

Prepared for

HIGH ALTITUDE POLLUTION PROGRAM

U.S. DEPARTMENT OF TRANSPORTATION
FEDERAL AVIATION ADMINISTRATION
Office of Environmental Quality
Washington, D.C. 20591

Technical Report Documentation Page

1. Report No.	2. Government Accession No.	3. Recipient's Catalog No.
FAA-EQ-78-05		

4. Title and Subtitle
Determination of NO_2 Photolysis Parameters for Stratospheric Modeling.

5. Report Date
June 1978

6. Performing Organization Code

7. Author(s)
John E. Davenport

8. Performing Organization Report No.
43p.

9. Performing Organization Name and Address
SRI International
333 Ravenswood Avenue
Menlo Park, California 94027

10. Work Unit No. (TRAIS)

11. Contract or Grant No.
DOT-TSC-1284

13. Type of Report and Period Covered
rept.
Final July 1976 - June 1978

12. Sponsoring Agency Name and Address
High Altitude Pollution Program
U.S. Department of Transportation
Federal Aviation Administration
800 Independence Avenue S.W.
Washington, D.C. 20591

14. Sponsoring Agency Code

15. Supplementary Notes

16. Abstract

17. Key Words	18. Distribution Statement
nitrogen dioxide, NO_2, photolysis, absorption coefficients, quantum yields, stratosphere, modeling	unlimited DISTRIBUTION STATEMENT A Approved for public release; Distribution Unlimited

19. Security Classif. (of this report)	20. Security Classif. (of this page)	21. No. of Pages	22. Price
unclassified	unclassified	43	

Form DOT F 1700.7 (8-72) Reproduction of completed page authorized

410 281

ABSTRACT

This study was undertaken to obtain photolysis parameters for the presence of NO_2 + hν → NO + O, which could be supplied to the modeling of that region.

The absolute absorption coefficients for NO_2 were measured at 297°, 247°, 226°, and 204°K and are tabulated at 1-nm intervals over the 390-420 nm photolysis cut-off region. Experimental uncertainties range from 2% at room temperature at 420 nm to 15% at 204°K, and mainly fall in the 4-7% range.

The quantum yield for NO production was measured at 300° and 223°K over the same wavelength range and at 5 nm intervals with an uncertainty of about 11%. The photolyses were carried out at pressures as low as 4.5 millitorr NO_2 in a well collimated long path multiple reflection cell in order to prevent significant N_2O_4 formation at low temperatures. About 5 torr nitrogen was used to prevent self-reaction via NO_2^* + NO_2 → 2NO + O_2. Photolysis of NOCl at room temperature was used as an actinometer.

Implications of the data concerning the detailed photolysis mechanism of NO_2 and stratospheric modeling of this process are briefly discussed.

CONTENTS

ILLUSTRATIONS

TABLES

ACKNOWLEDGMENT

The assistance of Bosco Lan, James Blessing, and Robert Sharpless in the construction of apparatus and the acquisition of data is hereby acknowledged. Discussions with Dr. Dale Hendry and Dr. Tom Slanger, along with the use of some of their equipment were helpful in resolving the NO monitoring system dilemma described in the report. Dr. Ted Mill has also assisted in this project by reviewing reports and by acting as project supervisor.

INTRODUCTION

Observations made over the last 30 years have made it clear that the simple Chapman mechanism for stratospheric ozone chemistry predicts about five times more ozone than is actually present in the atmosphere. Johnston (CIAP Monograph 1, 1975) has suggested that NO_2 concentrations of about 10^9 molecules cm^{-3} of NO_2 in the ozone-formation region from 20 to 30 km are sufficient to account for most of the discrepancy, primarily through the cycle.

$$NO_2 + O \rightarrow NO + O_2 \quad (k = 9.1 \times 10^{-12}\ cm^3\text{-molec}^{-1}\ sec^{-1}) \tag{1}$$

$$NO + O_3 \rightarrow NO_2 + O_2 \quad (k = 9 \times 10^{-13} \exp(-1200/T)\ cm^3\ molec^{-1}\ sec^{-1}) \tag{2}$$

$$\text{Net:} \quad O + O_3 \rightarrow 2O_2 \tag{3}$$

where reaction (1) is the rate-controlling step at these altitudes. Photolysis of NO_2:

$$NO_2 + h\nu\ (\lambda \lesssim 400\ nm) \rightarrow NO + O \tag{4}$$

competes with reaction (1) for the NO_2. The rate constant for process (1) is from Davis et al. (1973), and the rate constant for process (2) is from Hampson and Garvin (1973).

At lower elevations, however, NO_2 photolysis acts as a source of ozone. After reaction (4), ozone is formed by recombination:

$$O + O_2 + M \rightarrow O_3 + M \tag{5}$$

Thus, modeling of the effects of trace amounts of NO_2 in the stratosphere is necessary to accurately characterize the ozone balance there. More important, we must understand this aspect of the problem before we can predict the effect of artificial injection of nitrogen oxides on stratospheric ozone concentrations.

To obtain the data necessary to model NO_2 photochemistry in the stratosphere, our specific objectives were, first, to measure the absorption cross section of NO_2 as a function of wavelength from 390 to 420 nm over a temperature range of about 200-300°K, and second, to measure the quantum yield of products significant to stratospheric chemistry (NO + O) in the photolysis of NO_2 over the same wavelength and temperature ranges.

BACKGROUND

The kinetic rate coefficients affecting the concentration of NO_2 in the stratrosphere are fairly well known over temperature ranges appropriate to the stratosphere. However, the absorption cross sections and photodissociation quantum yields (both as a function of wavelength) for the process

$$NO_2 + h\nu(\lambda < 398 \text{ nm}) \rightarrow NO + O \qquad (4')$$

have not yet been measured in this temperature region except for the recent data by Bass et al. (1976) published during the course of these experiments. Especially important is the quantum yield in the photolysis cut-off region around 398 nm.

Bass et al. (1976) gave NO_2 extinction coefficients in the spectral range from 185 to 410 nm and 298°K and 235°K. Although they did not study the quantum yield behavior for the critical photolysis threshold region (390–420 nm), examination of these data in the 397 to 410 nm region shows that the extinction coefficients at absorption peaks are reduced much less than in absorption valleys, where they are reduced by about 5% to 15%. This effect was expected since the dissociation wavelength of 397 nm precludes any but bound transitions above that wavelength, which implies that the difference in absorption intensities as a function of temperature must be due to rotational population shifts, as well as to shifts in thermal translational energy. Vibrational population changes are not expected to be large because at room temperature most of the populations are the $v'' = 0$ level. In fact, the data of Bass et al. do not show any large changes with temperature that could be attributed to vibrational population shifts in the 390 to 410 nm wavelength.

The quantum yield, however, has not been measured below room temperature. The measured quantum yields for NO production at room temperature show values less than unity below the photolysis threshold, only 0.9 at 377.9 nm, for instance (Jones and Bayes, 1973). Fluorescence yield and lifetime measurements indicate that the remaining 10% may form an NO_2^* species that radiates or reacts when it is not quenched by an inert gas. Furthermore, evidence from O^{18}

scrambling experiments implies O-atom production in pure NO_2 at discrete wavelengths as long as 412 nm (Jones and Bayes, 1973). Most of the NO yield and O-atom yield in the 390-420 wavelength region can be explained by the thermal energy distribution among rotational levels of the ground state. However, according to Jones and Bayes (1973) and Uselman and Lee (1976) and Lee and Uselman (1972), NO_2 and O_2 quantum yields are not totally explained by ground-state internal energy considerations.

The only study on the temperature dependence of NO_2 photolysis (Pitts et al. 1971) is of little direct use for stratospheric modeling since the work was done under conditions very much different from those in the stratosphere. The studies were conducted at temperatures above 293°K and at NO_2 concentrations higher than those found in the stratosphere.

Thus, despite the crucial role of NO_2 in the chemistry of the stratosphere, no complete determinations of NO_2 quantum yield and absorption data are available that would permit accurate calculations of the stratospheric NO_2 photolysis rate in the fall-off region. Laboratory measurements of the NO_2 photolysis quantum yield and absorption cross section are complicated primarily by

(1) The large enthalpy of reaction for $2NO_2 = N_2O_4$ [ΔH° = 13,639 cal $mole^{-1}$ K^{-1} (Stull and Prophet, 1971)], which drives the equilibrium to the right as temperature is decreased,

(2) Formation of relatively stable (lifetime up to 120 μsec) electronically excited NO_2 species that may react with ground-state NO_2 molecules in the laboratory, but are either quenched or radiate in the stratosphere.

In the current study, the temperature effects on the $2NO_2 = N_2O_4$ equilibrium were offset by working at NO_2 pressures down to the micron range. The data of Bodenstein and Boes (1922) as modified by Stull and Prophet (1971) were used to ensure that N_2O_4 was always less than 1% of the NO_2.

Self-reaction was limited by working at low NO_2 pressure and high N_2 pressure. For instance, we calculate that the mean collision time for NO_2 at 1 millitorr pressure and 298°K is 124 μsec, compared with a radiative lifetime of abut 120 μsec at room temperature. However, self-reaction can be effectively controlled by using well-characterized NO_2 quenchers such as CF_4 and N_2 (Jones and Bayes, 1973).

ABSORPTION COEFFICIENT MEASUREMENTS

Details of Apparatus

The basic apparatus used to measure the NO_2 absorption coefficients is shown schematically in Figure 1. In general, it consisted of a tungsten-halogen lamp, regulated lamp power supply, and monitoring system; a gas purification, mixing, and pumping system; a Perkin-Elmer "40 Meter" multiple-reflection Whilte cell; an ethylene glycol cooling and circulation system; and an MPI 1018B monochromator.

Two light sources were actually used. A 175-watt tungsten lamp was used to obtain room temperature data where high NO_2 pressures could be used and only three reflections were necessary to obtain very good absorption intensity. A 1000-watt quartz-halogen lamp was used to measure the absolute absorption coefficients at other than room temperature. The power was regulated to within 1% and the lamp encased in a metal housing to prevent air currents from disturbing the skin temperature and thus the intensity stability. A monitor, based on a 1P28 photomultiplier, was adjusted so that it could easily detect a change of 0.1% in the overall lamp intensity. After an initial period of about 10 to 15 minutes, the lamp intensity rarely varied this much over an 8-hour period except when near the end of the lamp lifetime.

The gas-handling system consisted of three parts: a stainless steel gas inlet system, a glass distillation and storage system with Teflon stopcocks, and a copper and rubber tube exhaust system. Pressures were measured with a Texas Instruments (TI) Bourden cell gauge for most experiments down to 50 millitorr; a transducer was used at pressures down to 10 millitorr. Both systems were standardized against McCloud gauges. The TI gauge had an uncertainty of less than ± 10 millitorr at all pressures used, and the transducer precision was about ±1%.

The Perkin-Elmer multiple-reflection White cell, with 15-cm main optics, was modified for use on this project. The mirrors were stripped of their gold coating and an aluminum coating was vacuum deposited. We then applied a protective SiO_2 overcoat, which is inert to the NO_x and other gases expected to be present during these experiments. The maximum path length was limited to 20 meters in the absorption coefficient measurements by the combination of surface reflectance, light intensity, and detector sensitivity. The total

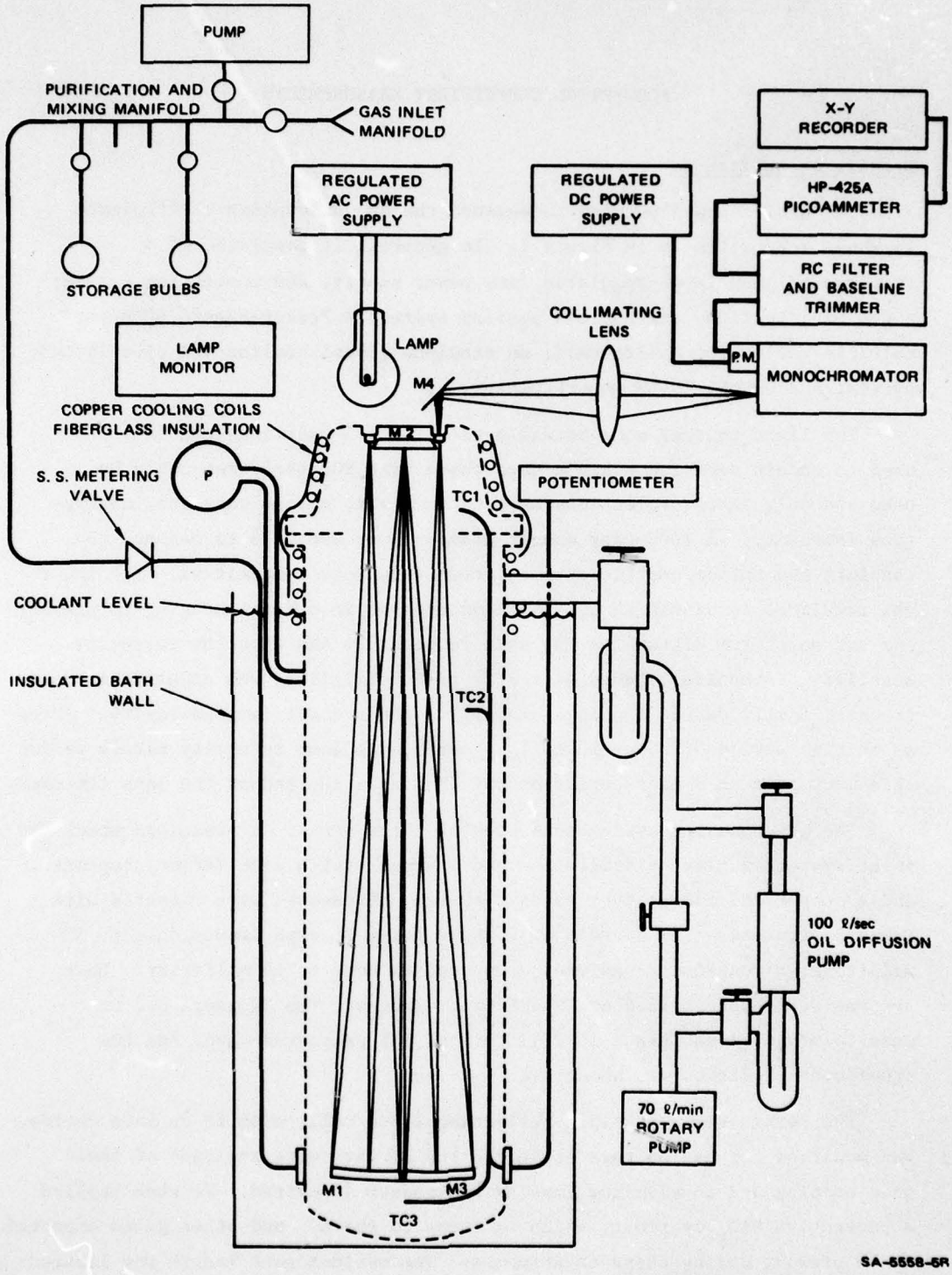

FIGURE 1 APPARATUS USED IN MAKING ABSORPTION COEFFICIENT MEASUREMENTS

Used for absorption data taken over 398-cm path length. M1, 2, 3, 4, are system mirrors in order of light incidence. TC 1, 2, 3, represent thermocouple leads.

path lengths in the cooled Perkin-Elmer system were measurable to within 1% by direct measurement. This uncertainty includes the slight difference in path lengths for light striking the edges and the center of the lower mirrors. Inlet and outlet apertures were 5-mm wide; the sealing gaskets were made of Viton.

The reaction cell was placed in a 50-gallon insulated cooling bath, deep enough to immerse about 85% of the cell. The other 15%, with the input optics, was cooled with coils through which the bath liquid was circulated. At -69° it was found convenient to pack the top with dry ice to maintain the internal temperature.

Cooling bath equipment also included a 60-gal/min circulation pump, a 500-ml/min diastolic pump for the cooling coils, and a cooling bath capable of cooling the system to 273° overnight without using dry ice or liquid nitrogen. The coolant selected was 70% ethylene glycol in water. This mixture remained liquid down to around 198°K, measured outside the photolysis cell. Temperatures inside the cell were measured using three thermocouples: one at the bottom of the cell, one at about the liquid level, and one at the uppermost portion of the cell.

The light from the lamp was passed directly into the entrance aperture through a 6-mm plate Pyrex window, traveled through the multiple reflection path, and passed back out through another 6-mm Pyrex window of the exit aperture. Dry nitrogen was passed over both windows to prevent condensation of atmospheric moisture. After ixiting the cell, the light was reflected by a plane mirror through a condensing lens, which focused it on the salt of an MP-1018D 0.45-meter scanning monochromator. The grating used in these experiments was a 2360-grooves/mm Jarrell-Ash replica grating. Since the grating was used in second order, a Corning 4-73 filter was used to cut off 800 nm of radiation, which could otherwise have reached the photomultiplier.

A 1P28 photomultiplier detection system, including a DC power supply, an HP 425A picoammeter, and an X-Y recorder, was used to measure the intensity of the emerging light beam. The wavelength resolution of the system using 10-μm slits was better than 0.037 nm, based on measuring the full width at half maximum of the 365.48-nm line from a low-pressure mercury source.

For the preliminary runs at room temperature, we planned to use a standard mixture that would make measurements more accurate and precise and also duplicate atmospheric densities and pressures. However, the mixture ordered from Linde Gas Company was observed to decrease in $[NO_2]$ from 0.54% to 0.312% as derived from absorption measurements at 400 nm. The rate of decrease in the concentration was not first order in NO_2, since the percent disappearance with time is estimated to have decreased in about one-third its value when analyzed 1.5 months before the final determination. This changing concentration made it necessary for us to purify and mix our own materials.

The NO_2 (99.8% minimum purity) was obtained commercially (Matheson Company) and purified in the usual way by reaction with excess O_2. The O_2 was pumped away and the purified NO_2 allowed to sublime from the purification bulb at $0^{\circ}C$ into the storage bulb trap at $-78^{\circ}C$. The white cubic crystals that formed were easily separated from the glass walls by light tapping. After the pressure was adjusted to the desired value, the NO_2 was recondensed and N_2 (Matheson -99.9% minimum purity) added to one atmosphere. Mixtures made from pure NO_2 contained less than 0.1% NO as determined in the resonance cell described later.

When the mixtures were stored in the darkened glass bulb, the present NO increased at a rate of about 0.37% of the NO_2 per day, while the NO_2 decreased at a slightly higher rate, about 0.5% per day. Evidently, small amounts of NO_x impurities such as N_2O_3, N_2O_5, or HNO_3 were being formed. Thus, only freshly prepared mixtures were used for the absorption measurements after at least 8 hours were allowed to complete though mixing.

Measurements of the rate of decay of NO_2 in the mixture showed that, once the mixture was in a conditioned cell at 25 torr total pressure and about 100 millitorr NO_2, the optical absorption decayed at a rate slower than 1% in 30 minutes. By contrast, the initial rate of disappearance for NO_2 in an unconditioned cell was much higher; initial rates as high as 5% per minute were observed under the same conditions. Presumably this decay was due to reaction with cell water vapor to form HNO_3, which does not measurably absorb in the 400-nm region. At any rate, conditioning the cell at about one torr of NO_2 overnight eliminated the problem of high NO_2 disappearance rates in the photolysis cell. Thus, at least at these low NO_2 pressures, NO_2 destruction in the conditioned cell was not fast enough to affect the results of the absorption coefficient measurements.

Procedures

The procedures were essentially the same at all temperatures. After the reaction cell was pumped down to less than 10^{-4}, the system linearity was checked, as well as the NO_2 destruction rate in the cell. This was accomplished by first measuring the absorption as a function of pressure at a monochromator setting of 4.00.0 nm, which was actually 399.77 nm. A flowing system was used to take these intensity measurements as the pressure was increased stepwise. Then the system was stepwise pumped out, resulting in I_o/I static measurements at the same pressures as used in the flowing system measurements. The plot of log I_o/I as a function of total pressure in Figure 2 established the linearity of the measured photocurrent with transmitted intensity. In addition, there was no significant difference between the absorption measurements for a flowing system and the static system, which indicated that any unexpected gradients would nto affect the measurements done in a flow system made, and that significant destruction of NO_2 did not occur in the static measurements. This check was carried out at each temperature, and in each case a static system could be used to obtain precise and linear data.

Several runs were made over the same region with at least three different electronic filtering time constants ranging up to 2 seconds to be sure that no spurious peaks appeared and no absorption features were obliterated. A lamp monitor was used to be sure the lamp intensity did not vary more than 1% during each run. However, because of drift in the electronics, it was necessary to reset initial conditions and begin a retrace. If there was more than 0.5% shift in the measured intensity, the run was not used and the scane was repeated.

For the data at (204°-69°C) where 40 passes were needed due to the low NO_2 pressure, a digital multichannel scaling system was used to improve the signal-to-noise ratio. The Canberra Model 8100 multichannel scaling system took the place of the time-filtered picoammeter system. Each scan was made under the same conditions as with the picoanmeter system except that five scans were summed. The MCS resolution was 4000 channels for 30.0 nm or 133 channels/nm. The accumulated signal was recorded permanently using an X-Y recorder after obtaining digital values for the counts in several key channels. The background intensity was recorded the same way. Correction for the higher count-rates at the longer wavelengths was applied according to

$$R = \frac{1}{1 - R_o\tau} \qquad (6)$$

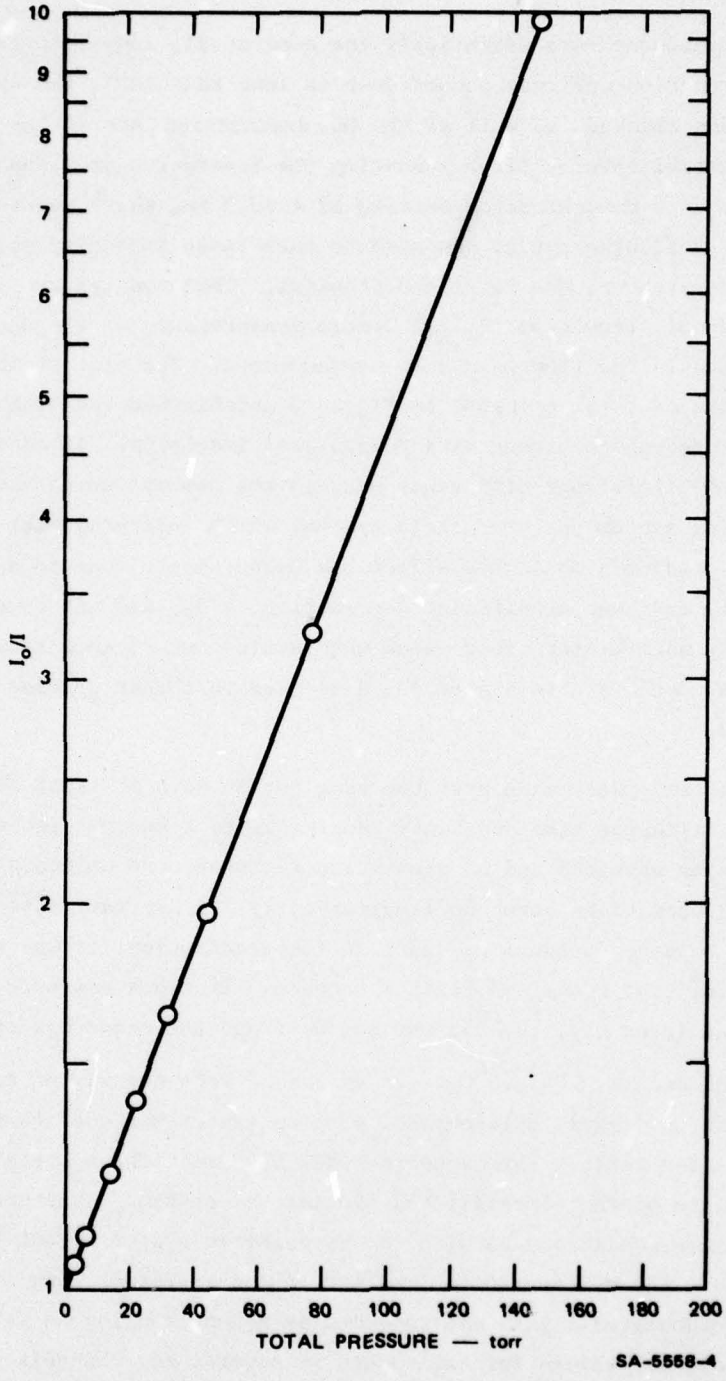

FIGURE 2 LINEARITY OF SYSTEM RESPONSE

Data points taken at 399.77 nm in both flowing system, as pressures were increased, and static system as gas was successively pumped out over a 15-minute period. Total pressure given is for a nominally 0.5% NO_2 mixture. Each data point represents two measurements, one at the given pressure in the following system, and one in the static system.

where R is the real count, R_o is the rate equivalent of the counts observed in the 3-second channels, and τ is the counted pulse deal time (1.1 μsec in case).

Results

Table 1 summarizes the experimental conditiions for the absorbtion coefficient measurements. Figure 3 shows the first survey scan, which was taken near room temperature (300°K) at 19.6 torr total pressure with an NO_2 pressure of 0.085 torr. The figure clearly shows the overall relations of the parameters involved in making individual measurements, but it is not very useful for measuring the absorbance because of the low sensitivity at short wavelengths. Better values for absorbance were obtained from data such as that in Figure 4, because the increase in lamp intensity with wavelength is more nearly linear over shorter wavelength segments and because the vertical scale is expanded. The values obtained for the extinction coefficients were calculated from:

$$\alpha = \left[\frac{\ln(I_o/I)}{\ell\ P_{NO_2}}\right]\left[\frac{273.16}{T}\right] \qquad (7)$$

and are shown in Table 2. In equation (7), I_o is the relative lamp intensity at a given wavelength, I is the transmitted intensity at the same wavelength, ℓ is the path length, P_{NO_2} is the above pressure of NO in atmospheres, T is the absolute temperature.

Table 1

SUMMARY OF CONDITIONS FOR ABSORBTION COEFFICIENT MEASUREMENTS

Temp. (°K)	297°K	277°K	247°K	226°K	204°K
Temp. Uncert. (°K)	± 1	± 1	± 1	± 2	± 2
Path Length (cm)	3.98	3.98	11.9	11.9	39.7
Pressure NO_2 (Millitorr)	78	54	11.3	2.1	.32
Total Pressure (Torr) Calculated	21.3	18.3	22.4	21.5	16.3
Fraction of NO_2 as N_2O_4	0.00	0.00	.01	.06	.10
Slit Width (micrometers)	10	10	30	30	100
Band Pass (nm)	.04	.04	.11	.11	.38
Estimated Precision On I/I_o					
At 390 nm	± 5%	± 6%	± 8%	± 9%	± 15%
At 400 nm	± 4%	± 4%	± 5%	± 6%	± 8%
At 420 nm	± 2%	± 3%	± 3%	± 4%	± 6%

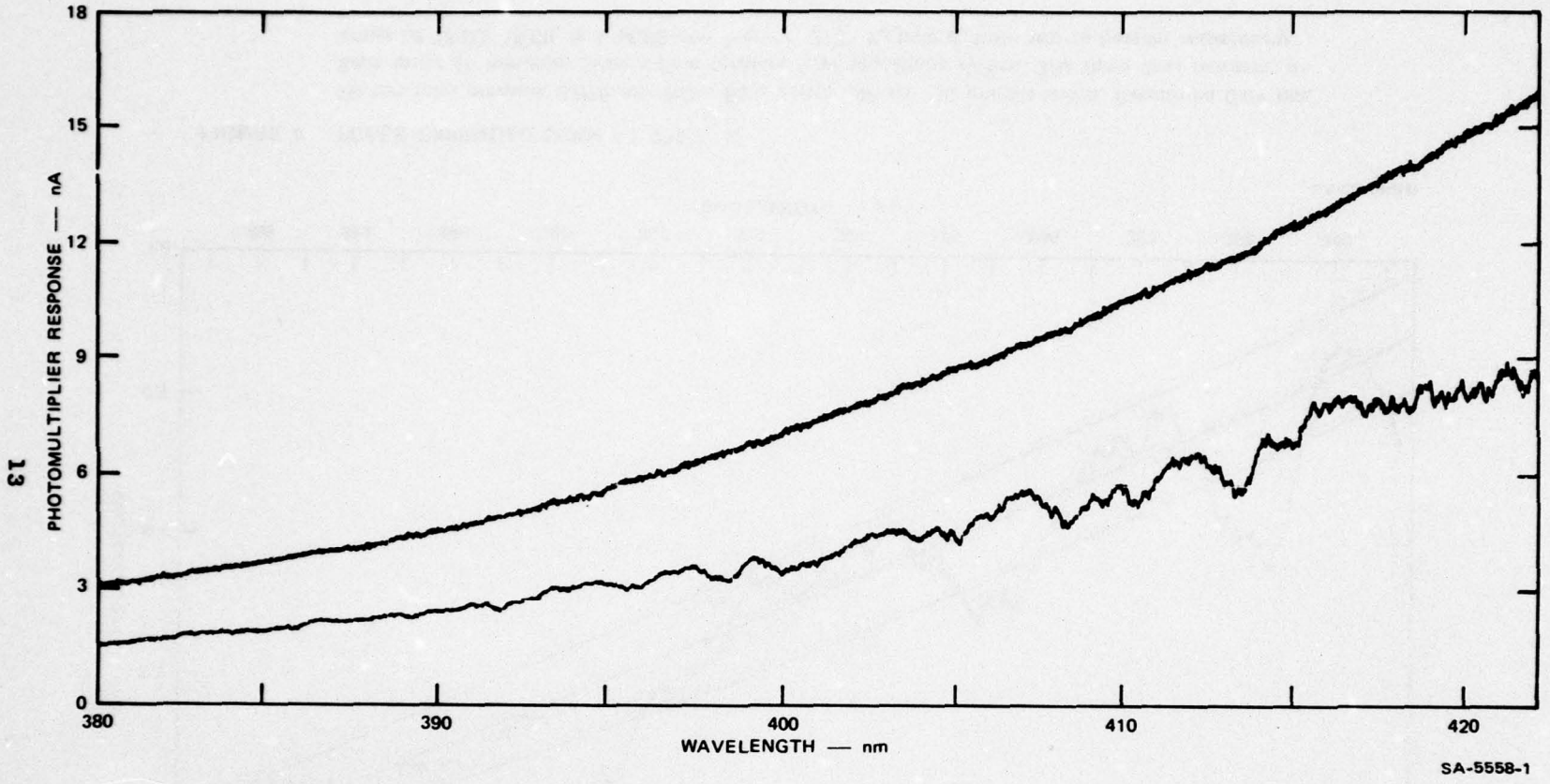

FIGURE 3 SURVEY SCAN AT 300.0°K

Top curve, incident intensity. Bottom curves taken with a flowing 19.6-torr, NO_2 in helium mixture. The pressure of NO_2 was 0.085 torr. Slit width 25 μm. Scan speed 1.0 nm min^{-1}. System time constant 2 sec.

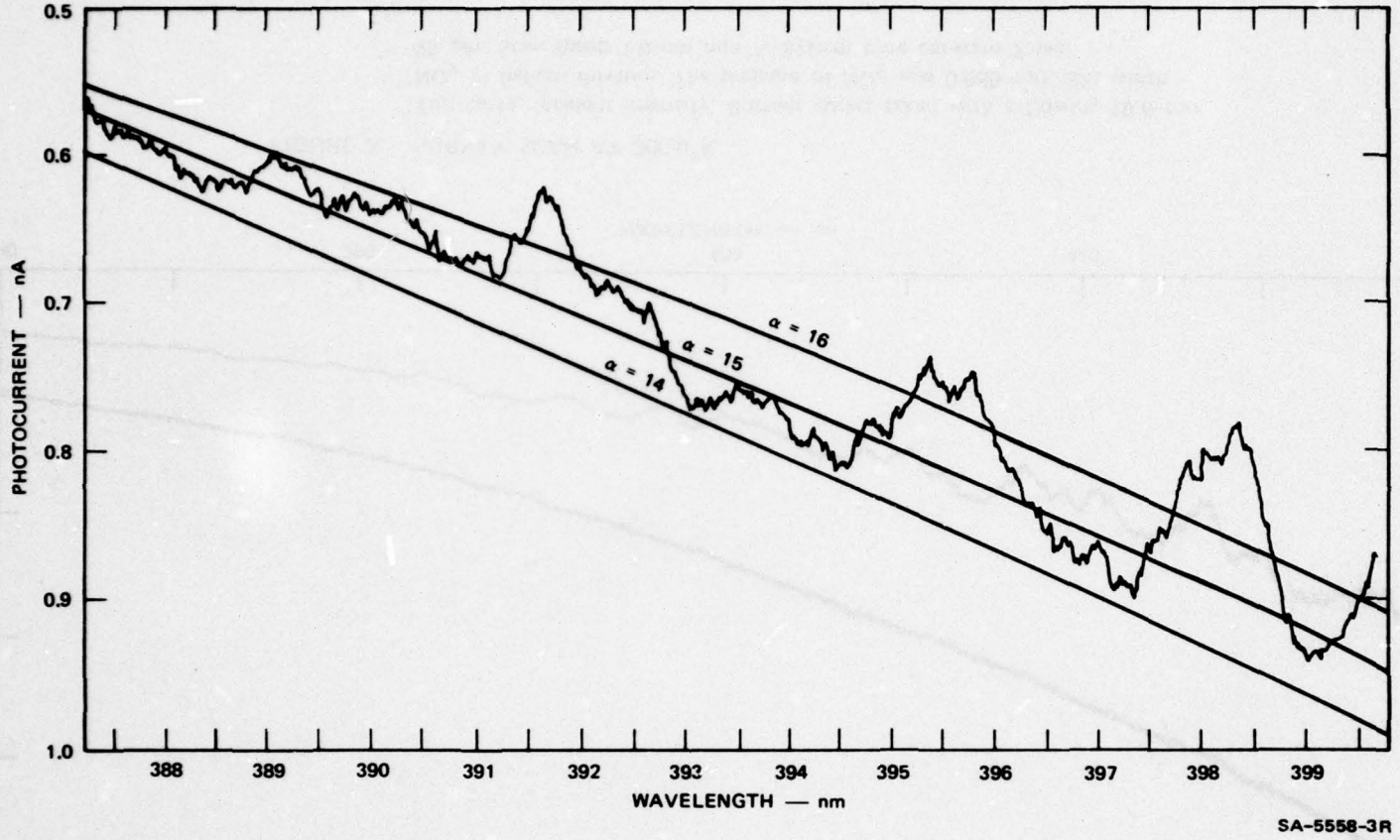

FIGURE 4 SCALE-EXPANDED SCAN AT 276.7° K

20 ton total pressure. 0.076 torr NO_2. Path length 398 cm. 10 μm slit width. Resolution 0.04 nm. Scan speed 25 mm/min. System time constant 0.47 sec. Static system. The three lines represent a values of 16.00, 15.00, and 14.00 atm^{-1} cm^{-1}, 273° K, base e, from top to bottom respectively.

Table 2

ABSOLUTE ABSORPTION COEFFICIENTS FOR NO_2 AT 390–420 NM FROM 204–297 ^{o}K

Wavelength (NM)	297 ^{o}K	277 ^{o}K	247 ^{o}K	226 ^{o}K	204 ^{o}K
390	16.5	15.7	14.4	14.6	14.0
391	16.3	15.3	14.8	14.3	15.0
392	17.1	15.6	16.4	16.5	15.8
393	15.0	14.4	14.7	14.1	12.9
394	15.4	14.9	14.7	14.1	13.9
395	16.1	16.2	16.1	15.3	14.9
396	17.4	16.2	15.9	15.3	9.5
397	15.3	14.5	15.7	12.4	12.8
398	17.3	17.4	17.9	17.7	8.3
399	15.6	14.5	13.9	13.4	17.5
400	18.6	19.7	16.9	16.4	18.8
401	17.7	16.8	17.3	16.0	19.1
402	15.7	14.5	14.7	14.6	16.7
403	14.7	13.4	13.1	12.6	13.3
404	17.1	15.9	16.3	14.7	14.3
405	17.2	16.5	16.4	15.7	14.0
406	15.4	14.0	13.6	13.0	16.4
407	13.3	12.2	10.9	10.6	10.6
408	16.8	15.5	11.9	14.3	17.1
409	17.1	15.1	18.0	13.4	13.0
410	16.2	14.8	14.6	13.9	13.3
411	16.0	15.5	15.1	15.2	14.2
412	14.8	13.6	13.9	12.9	13.3
413	19.3	18.5	18.8	17.4	16.0
414	14.3	13.6	14.4	12.0	11.8
415	16.6	16.0	14.9	15.6	14.2
416	13.3	13.7	10.9	13.1	8.4
417	14.6	13.8	11.3	11.0	10.5
418	14.9	14.5	14.0	11.1	12.8
419	15.0	13.5	16.0	12.6	12.5
420	15.9	15.5	14.3	13.4	12.2

Values in columns are values for α in cm^{-1} atm^{-1} reduced to ^{o}C, base e

QUANTUM YIELD MEASUREMENTS

Equipment Modification and Procedures

The apparatus used for measuring the NO_2 photolysis quantum yields was basically the same as that used for measuring the absorption coefficients, except for three changes: the mirrors in the cell were resurfaced with five layers of dielectric to increase the reflectivity, the halogen-tungsten light source was replaced by a xenon lamp/monochromator combination and NO concentration analysis cell was added. Figure 5 diagrams the additions to the apparatus. A 32.0-meter path was used throughout the photolysis experiments.

The original mirror surfaces had lost considerable reflectivity over several months, since it had proved necessary to clean off matter that deposited on clean surfaces of the two lower mirrors after every repressurization. The dielectric layering greatly improved the reflectivity of each surface from 0.85 to 0.98 at 405 nm. Unfortunately, the reflectivity at 390 nm was not improved so that after 10 reflections the intensity exiting the cell was less than 10% of that at 420 nm. This made data more difficult to obtain at short wavelengths since they required longer photolysis times.

The light source used in the quantum yield experiments consisted of a Hanovia 795C-394, 2500-watt, high-pressure xenon lamp. It was housed in an Oriel Model 6153 Universal lamp housing with 100-mm quartz optics. The regulated power supply was adjusted to provide 2100 watts for all experiments. After an initial warmup period of about 10 minutes, the observed intensity did not change more than 1% in any period up to 10 hours of continuous use. The light from the lamp was passed through a 10-cm water-cooled liquid filter. Besides blocking the intense infrared radiation with ultrapure water (obtained via a reverse-osmosis process), we used $CuSO_4$ (0.44 g in 100 cc of 7 M NH_4OH) to attenuate intense lamp radiation at wavelengths longer than 420 nm, which could have heated the slit enought to distort it.

The light emerging from this filter was then focused on the 100-μm slit of a Jarrell-Ash Model 82-410, 0.25-meter Monochromator with a 64 x 64 nm grating having 2365 grooves mm^{-1} and blazed for 300 nm. The aperture ratio was f/3.5 and the resulting resolution was 0.34 nm based on the full width at half maximum at the 366 nm line from a low-pressure mercury source. The emerging monochromatic radiation was then passed through a cylindrical condensing lens, through the Corning 4-73 filter, and then into the White cell entrance aperture.

The third addition to the apparatus was an NO analysis system (See Figure 5). This system had its own diffusion and rotary pumps as well as its own inlet manifold. The system was connected to the same Texas Instrument precision pressure gauge that was used to measure reaction cell pressure. The resonance cell itself was connected to the main reaction cell through 3/8-inch tubing. It consisted of a 2-liter all-quarter cell with three mutually perpendicular optical axes, of which only two were used. One optical path was used for the resonance lamp radiation; the window was 20 cm from the center of the cell to minimize scattered light. The other was used to detect the fluorescence radiation and was 10 cm from the center of the cell.

The resonance lamp consisted of a 12-mm glass tube, perpendicular to a quartz window through which either air or NO in a helium carrier flowed through a 100-watt microwave discharge at about one torr total pressure. The total path through the cell to the cooled 1P28 photomultiplier was about 30 cm. Both windows were opposed to Wood's horns to help minimize scattering of resonance radiation directly into the photomultiplier apperture. Finally, the outer walls of the cell were painted black and wrapped in opaque metal foil. The volume of the cell was approximately 2 liters.

Before entering the cell, the resonance radiation emitted from the lamp passed through a Pomfrit Research Optics Model 20-2100-1 interference filter centered at 216.2 nm with a band pass of 13.5 nm. It then directly entered the cell and traveled to the scattering region. As it passed out the exit window, the fluorescence radiation was again filtered through an ARC Model 220-N filter with a peak wavelength of 219.5 nm and a 25.0 nm bandwidth.

The spectrum of the lamp emission (Figure 6) shows that the specific transitions involved in the resonance system were the (0←0) γ-system and the (0←1) γ-system. A dry-ice-cooled 1P-28 photomultiplier at 700 volts was used to monitor the fluorescence intensity. Signals as low as 0.01 nA could be separated from the 0.05-nA noise level with 2-sec RD filtering.

Much effort was spent in developing this [NO] analysis system, and an alternative system was evaluated. From our past experience with NO resonsnace systems, both fluorescence and absorption, we originally felt that resonance absorption measurements should be used to determine the [NO] product concentration. To test the absorption method, we made resonance absorption measurements with a 0.8-meter absorption cell. The results (see Table 3)

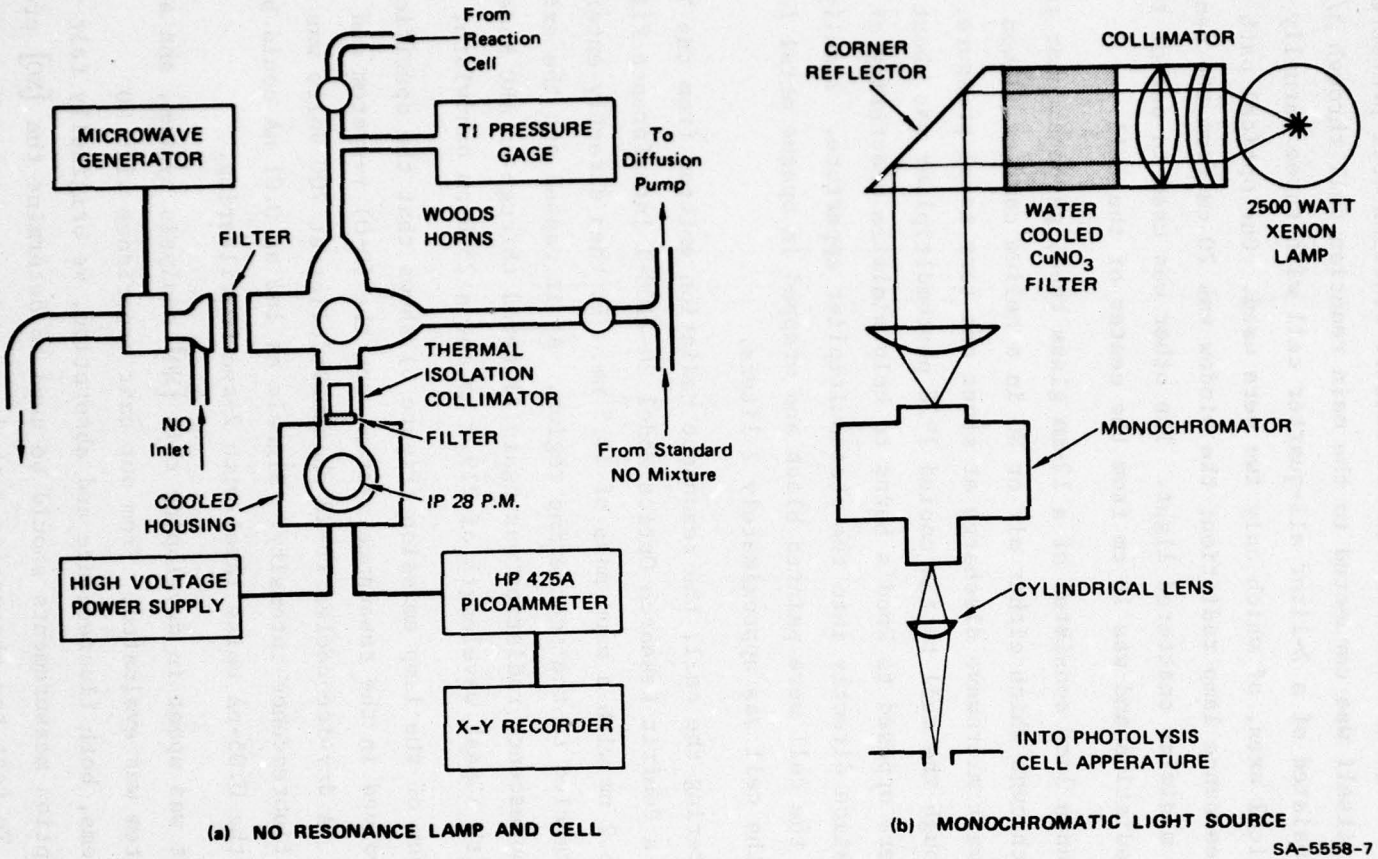

(a) NO RESONANCE LAMP AND CELL

(b) MONOCHROMATIC LIGHT SOURCE

SA-5558-7

FIGURE 5 APPARATUS ADDED TO MAKE QUANTUM YIELD MEASUREMENTS

The resonance fluorescence system (a) was teed into photolysis pressure measuring manifold (see Figure 1). The monochromatic light source took the place of the incandescent lamps in Figure 1.

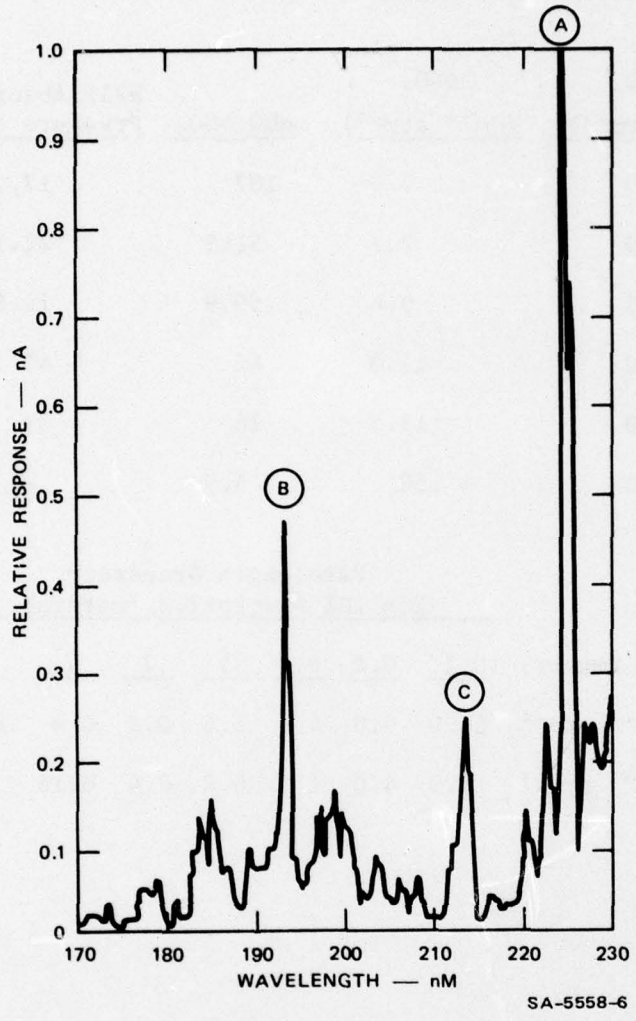

FIGURE 6 NO RESONANCE LAMP EMISSIONS

8 millitorr NO, 2.0 torr Ar. Made with a Jarrell-Ash 1/2-m Seya-Namioka scanning vacuum spectrograph with a resolution of 1.5 nm at the slit width used (50 m). The labeled peaks represent the following transitions: A is the v' = 0 to v'' = 0 transition of the γ system; B is the v' = 3 to v'' = 0 transition of the δ bands (the shoulder degraded to short wavelengths corresponds to the v' = 3 to v'' = 2 transition of the γ system); and C is the v. = 1 to v'' = 0 transition of the γ band system.

Table 3

NITRIC OXIDE RESONANCE ABSORPTION DATA

Assignment	αNO (cm^{-1} atm^{-1})	αNO_2 (cm^{-1} atm^{-1})	$\alpha NO/\alpha NO_2$	Half Absorption Pressure (Torr)	λ (nm)
$\varepsilon_0 + \gamma_4$	750	7.0	107	17.2	187.7
ε_0	400	7.7	51.9	22.2	191.2
γ_2	575	9.6	59.9	19.9	204.7
γ_1	510	11.0	46	$\sim$ 45	214.9
γ_0	210	12.5	16	29	226.4
ε_1	850	$\sim$ 150	5.7	--	179.6

	Pathlength Necessary For 10% Absorption (meters)						
At pressure (mtorr)	0.1	0.2	0.4	1	2	4	10
α = 500 cm^{-1} atm^{-1}	16.0	8.0	4.0	1.6	0.8	0.4	0.16
α = 1000 cm^{-1} atm^{-1}	8.0	4.0	1.6	0.8	0.4	0.16	.08

show that the very poor sensitivity found using 0.1% NO in He at pressures up to 500 torr was in fact due to strong pressure broadening of the absorption peaks. (see Watanable et al., 1953). However, even at zero pressure, the absorption coefficient ncesssary for the low temperature experiments, about 1000 atm^{-1} cm^{-1}, was approached only by absorption in the ε_1 band at 180 nm and in the $\varepsilon_o + \gamma_4$ band at 188 nm, and these bands were greatly affected by pressure broadening of the absorption line shape. Table 3 gives the total pressure with added helium at which the absorption coefficient for these particular systems and others were half what they were at zero torr helium. The effect with nitrogen may have been greater. We thus concluded that the usefulness of resonance absorption was marginal for experiments at lower temperatures with reasonable path lengths. Path lengths needed for 10% absorption are summarized in Table 3 for 500 and 1000 atm^{-1} cm^{-1}.

Since we found that the absorption coefficients were marginal even at low pressure, we decided to examine the sensitivity of an NO resonance fluorescence detector and to check for possible interference from NO_2. Table 4 summarizes the results of a series of experiments conducted with the resonance lamp used in the absorption experiments and with a general purpose resonance cell using various filters, phototubes, and NO and NO_2 concentrations. The signal per millitorr NO compared with the noise envelope showed an excellent signal-to-noise ratio. The lower sensitivity limit for 10% precision was about 0.05 millitorr, much better than the approximately 0.5 millitorr using the absorption method.

Thus the [NO] measuring system was built into the apparatus as described above, and 1% and 0.1% NO_2 mixtures, in O_2, were tested to determine the extent of NO_2 contribution to the scattered light signal. In these oxygen mixtures, any NO was quantitatively converted to NO_2 and, in contrast to the earlier experiments using the N_2 carriers, no signal was detectable over the total pressure range from 0.2 torr (0.20 millitorr NO_2) to 110 torr (1.10 millitorr NO_2). Later measurements in the nitrogen reaction mixtures showed that NO_2 photolysis was not measurable in a cell where the NO_2 residence time was less than 1 minute. It was also found that the lower limit for detection was considerably improved in the new cell: about 2-4 x 10^{10} molecules/sec (0.001 mullittor). Thus, the signals seen in the earlier NO_2 flow system must have been due entirely to an NO impurity in the NO_2 mixture used.

Table 4

NITRIC OXIDE RESONANCE FLUORESCENCE

Trial No.	NO Pressure (mtorr)	Fluorescence Signal (nA)	No Sensitivity $\left(\frac{nA}{mtorr}\right)$	NO_2 Pressure (mtorr)	Fluorescence Signal (nA)	No Sensitivity $\frac{nA}{mtorr}$	Background Signal (nA)	Noise Envelope (nA)	Sensitivity Ratio: NO/NO_2	Notes
1	0.22	33	46	--	--	--	240	0.3	--	NO filters
2	0.18	6.6	37	--	--	--	240	0.3	--	--
3	0.12	0.48	4.0	--	--	--	0.2	0.05	--	A
4	0.036	0.07	1.9	--	--	--	.14	0.01	--	B
5	0.30	2.6	8.7	--	--	--	.14	0.1	--	A
6	0.09	0.96	11	--	--	--	.14	0.1	--	A
7	0.39	6.3	16	1.35	2.4	1.78	.2	--	9.0	A
8	0.21	3.1	15	6.0	4.8	.08	.2	--	19	A
9	0.21	72	340	2.4	92	38.3	90	--	8.9	NO filters
10	1.05	1.4	1.3	9.1	.40	.04	.25	--	32	A
11	.39	4.0	10	9.3	2.8	.30	.25	--	33	A
12	0-10.0	0.00	0.00	--	--	--	--	--	--	C
13	0.30	159	530	2.2	120	54	--	--	9.8	NO filters
14	0.72	10	10	.75	4.2	5.6	--	--	1.8	D

Notes:

MgF_2-lamp window used instead of quartz. NO_2 measurements were made under same apparatus conditions as NO, after the NO was pumped out of the cell. Used 0.1% NO in He and nominal 0.39% NO_2 in He mixture described in text. Total pressure was kept at 10 torr in the reaction cell by adjusting argon flow rate. Detector based on 1P28 photomultiplier except for trial 14.

A. 216 nm interference filter, with 5.0 nm bandwidth, placed between lamp and fluorescence cell.

B. In addition to A., a 250 nm filter with 10 nm bandwidth placed between detector and cell.

C. Corning 9-54 filter used between lamp and cell.

D. Quartz disc between lamp and cell, solar blind photomultiplier.

Signal levels obtained using a standard 0.1080% NO in N_2 mixture are illustrated in Figure 7. The curvature at high pressures was due almost entirely to the effect pressure has on the NO absorption line shape. The same effect was noted in our study of resonance absorption methods for NO. Table 3 shows that the inert gas pressure (helium) at which the absorption coefficient was reduced to half its original value for the γ_o transition was 29 torr. With nitrogen, we found that the resonance fluorescence intensity was reduced to half its value in the resence of NO alone at 28 ± 1 torr N_2. The absorption and fluorescence data taken together imply that the effect is due to pressure broadening of the absorption line profiles.

This source of curvature in the intensity-versus-pressure curve necessitated either using a comparison system, comparing the intensity of the photolysed $NO/NO_2/N_2$ mixture with a standard 0.1% NO in N_2 mixture over a range of pressures, or using only low NO concentrations in the linear region. While either method would work, the comparison method offered the best way to obtain precise data since higher pressures could be used and larger signal levels obtained. The procedures used to obtain the final photolysis rate data was as follows. First, the second monochromator (still on the system from the absorption measurements) was used to check the intensity of light from the photolysis cell and the photolysis wavelengths. A shutter then blocked the light at the exit slit. Next, the reaction mixture was allowed to expand from the storage volume through a metering valve into the previously conditioned and evacuated photolysis cell. The shutter blocking the entrance slit of the photolysis cell was opened and I/I_o chcked, as in the absorption measurements, to determine the fraction of radiation being absorbed and to make sure of the $[NO_2]$. Usually, I/I_o was around 0.67%. Photolysis commenced at this point.

During this operation the resonance cell valve was left open. When the pressure had equilibrated, the resonance cell valve was closed and the resonance intensity was measured. The reaction mixture was then expanded into about three times the volume of the resonance cell and the intensity and pressure measured again. After the resonance cell was isolated, the expansion volume was pumped out with its own diffusion pump system, and the measuring process was repeated. Expansion and measurement cycles were usually repeated until less than 0.1 nA signal was obtained. The result was a plot similar to Figure 7. The standard 0.108% NO in N_2 mixture was then added to the completely

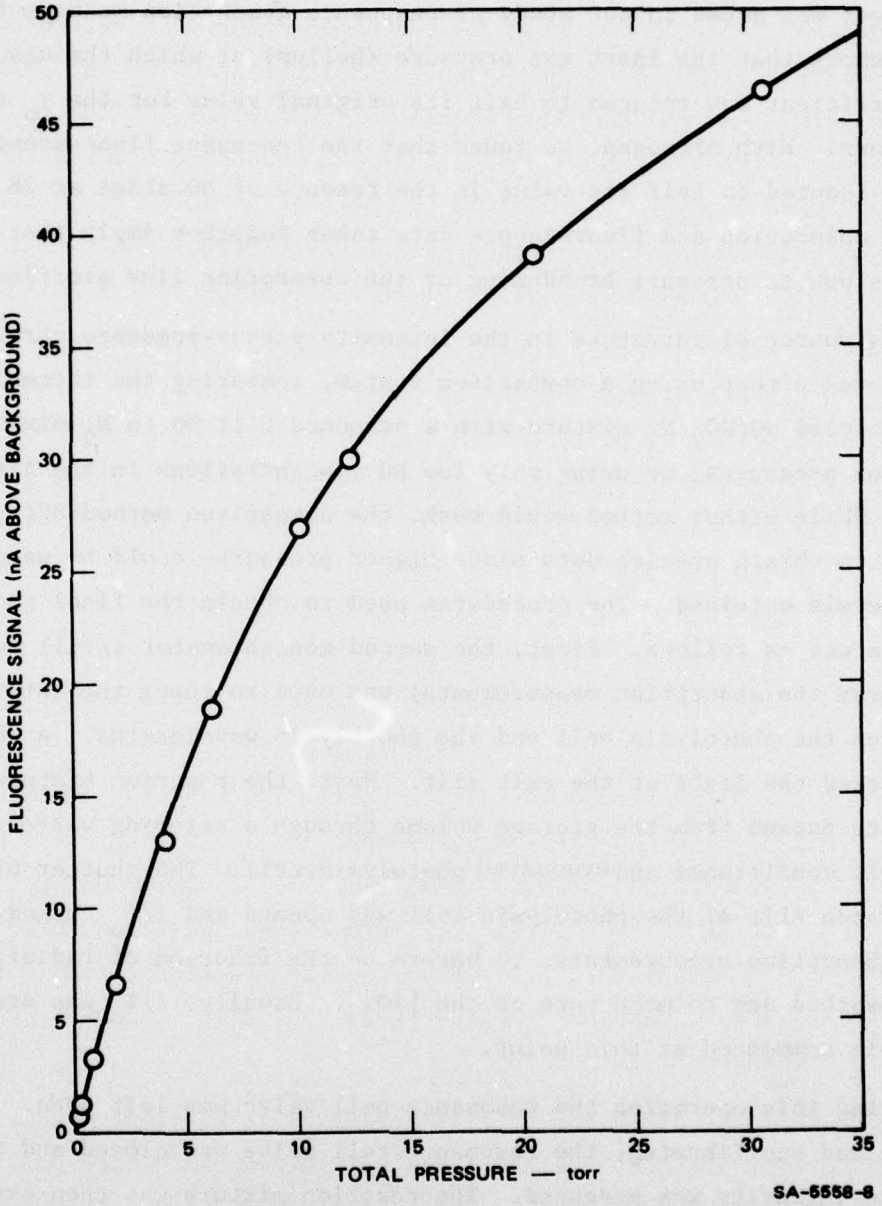

FIGURE 7 TYPICAL NO RESONANCE SIGNAL RESPONSE CURVE

Pressure is that of 0.108% NO in N_2 mixture. Photomultiplier: 700 volts, 1.2 nA background, 0.02 nA noise envelope. Initial slope = 4.33 nA per torr which corresponds to a sensitivity 4.68 nA/millitorr NO.

evacuated cell up to the total pressure of the reaction mixture. It, too, was withdrawn stepwise and the intensity noted as a function of pressures. The ratios of intensities at equal total pressures were compared to determine the ratio of NO in the reaction mixture to that in the standard, and thus to determine the [NO] in the mixture. Due to the NO absorption described above, small trends that appeared in the measured intensity ratios were resolved by plotting the ratios as a function of pressure and extrapolating to zero pressure. Corrections made in this way were always less than 12% and usually less than 5%. This procedure was followed several more times over the period of one to two hours, and the [NO] plotted as a function of time. The same procedure and standard were followed using nitrosyl chloride as an actionometer. The NOCl (Matheson 97% minimum purity) was distilled bulb to bulb between 0° and $-78^{\circ}C$, and then the reddish yellow solid was mixed with N_2 the same way as the NO_2. The lamp intensity through the cell was monitored so that the intensity attenuation exactly matched that of the previous run. This ensured that the extent of absorption of any scattered light would be the same for both NOCl and NO_2 photolysis. The Cl_2 formed in the NOCl photolysis did not measurably interfere with either the absorption of resonance radiation or fluorescence signal at the levels found in the photolyzed mixtures.

The photolyses were run three at a time at one wavelength. First either NO_2 or NOCl was photolyzed at close to $300^{\circ}K$. Then, dry ice was added to bring the cell temperature down to $223^{\circ}K$ and the NO_2 photolysis rate was measured again. Since the quantum yield of NO from nitrosyl chloride is not known to be 2.0 at low temperatures at the wavelengths studied, no actionometer run was made at the low temperature.

Destruction of NO_2 by dark reactions was determined to be typically 5.8×10^9 molecules sec^{-1} at 5.5 millitorr NO_2 initial pressure. This rate was averaged over 10 hours after a series of runs. The dark destruction rate was not usually significant compared with photolysis, but where it was, it was substracted. Similarly for NOCl, the dark rate at 1.30 millitorr was 8.2×10^9 molecules/sec.

Results

Figure 8 shows the results of a typical run following the procedures outlined above. The rates derived from separate runs (Table 5), such as illustrated in Figure 8, were used to obtain the final quantum yields given in Table 6. The quantum yield of NO production, ϕNO, at a given temperature and photolysis rate was derived from:

$$\phi NO = \frac{R_{NO}/2}{R_{NOCl}/Q_{NOCl}} \tag{8}$$

where ϕ_{NOCl} is the quantum yield of NO production from NOCl photolysis which is given by Kistiakowski (1930) and by Ashmore and Chanmugan (1953) as 2.0 over the entire visible and quartz UV regions of the spectrum. The ϕ_{NO} derived in (8) thus refers to the primary process and not the overall or experimental quantum yield, which is twice as large due to

$$O + NO_2 \rightarrow NO + O_2 \tag{9}$$

Propagation of error analysis based primarily on photolysis lamp intensity fluctuations of less than 3% over the 3 runs and detector precision of better that 4% leads to a determination of the experimental uncertainty of 10%, independent of wavelength and temperature except that at 390 nm, a significantly greater uncertainty in determining the lamp fluctuations occurred due to the low intensity levels there.

Table 5

EXPERIMENTAL CONDITIONS FOR NO_2 QUANTUM YIELD MEASUREMENTS

	Wavelength (NM)	Temperature (°K)	Initial Pressures PNO (Millitorr)	Initial Pressures PNOCl (Millitorr)	I/I_o	R_{NO_2} (Molecules Sec^{-1})	R_{NOCl} (Molecules Sec^{-1})
1.	410.1	299	5.6	132	.702	2.1×10^{11}	1.77×10^{12}
		222	5.2		.690	6.4×10^{10}	
2.	399.8	299	6.4	135	.635	6.1×10^{11}	9.6×10^{11}
		224	4.9		.631	5.4×10^{11}	
3.	395.2	301	6.2	102	.692	6.2×10^{11}	7.6×10^{11}
		223	4.7		.688	6.0×10^{11}	
4.	390.1	300	6.0	91	.680	2.4×10^{11}	3.2×10^{11}
		222	4.9		.696	2.3×10^{11}	
5.	420.8	301	5.8	154	.712	1.46×10^{11}	8.02×10^{12}
		223	4.5		.680	4.0×10^{11}	
6.	405.2	300	7.1	157	.636	4.1×10^{11}	1.38×10^{12}
		224	5.5		.637	3.6×10^{11}	

R_{NO_2} is the rate of NO appearance from NO_2 photolysis

R_{NOCl} is the rate of NO appearance from NOCl

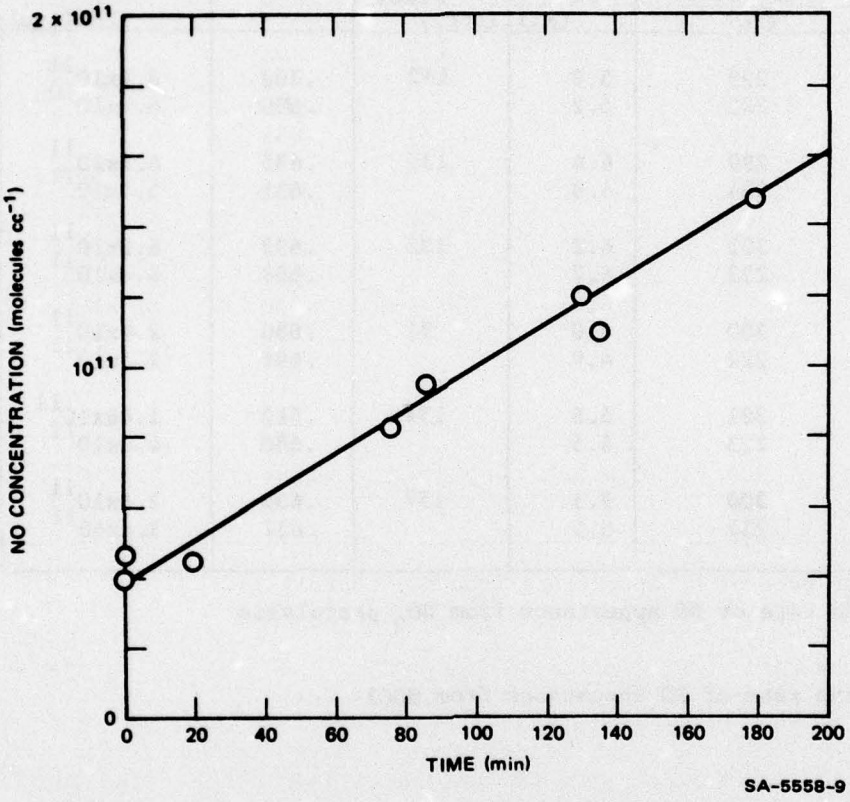

FIGURE 8 TYPICAL NO_2 QUANTUM YIELD DATA

NO_2 photolysis at 4.0 nm. Sampled NO concentrations as a function of time. Initial NO impurity equivalent to 0.19% NO_2. Initial pressure NO_2 = 6.4 millitorr.

Table 6

ABSOLUTE NO PRIMARY PHOTOLYSIS
QUANTUM YIELDS FROM NO_2 OVER THE RANGE
390-420 nm at 300°K and 223°K

At 300 ± 1°K Wavelength (nm)	390.1	395.2	399.8	405.2	410.1	420.8
ϕNO	0.75	0.82	0.64	0.33	0.12	.018
At 223 ± 2°K						
ϕ	0.74	0.79	0.56	0.26	0.041	.0053
Wavelength	389.8	395.1	399.4	405.2	400.2	419.7

DISCUSSION

The absolute absorption coefficients at room temperature, given in Table 2, agree well with the data in the literature. The value of Hall and Blacet (1952) average about 5-10% higher than the Table 2 values, while those of Johnston and Graham (1974) are only about 0-5% higher. The values presented in this report are slightly higher than the results of Bass, Ledford, and Laufer (1976), but actually overlap the data of Johnston and Graham and of Bass et al.

An early room temperature run (at 300.0°K) has been normalized to the data of Bass et al. at 400 nm. The relatively high degree of internal consistency between the two sets of data becomes apparent. This agreement is not surprising since, at room temperatures, large signal-to-noise ratios were obtained and the wavelength resolution used in these studies was the highest of the absorption coefficient measurements made. Also both were made under conditions that precluded the presence of N_2O_4. Most of the disagreement in Table 7 is caused by sharply fluctuating extinction coefficient values and by uncertainties in wavelength determination. For instance, the largest differences, 5.4%, was obtained at 409.9 nm, where α was determined to be 16.7 atm^{-1} cm^{-1} but Bass et al. list 15.9 atm^{-1} cm^{-1}. However, Bass et al. list a value of 16.8 atm^{-1} cm^{-1} at 408.875 nm, within our combined wavelength uncertainties. A similar example occurs at 396.0 nm, where the value listed by Bass et al., goes from 16.54 atm^{-1} cm^{-1} at 396.000 to 17.07 atm^{-1} cm^{-1} at 395.875 nm, compared with our value of 17.07 atm^{-1} cm^{-1}.

Thus the overall relative agreement is better than the absolute agreement and is well within our combined experimental error. The greatest source of error in these relative experiments was the approximately 3% uncertainty in I_o/I for any λ at room temperature. Propagation of error analysis indicates an overall ± 4% uncertainty in any data point presented in Table 7. This comparison indicates the general validity and precision of the data and the lack of noticeable interference from possible impurities present (such as HNO_2 and N_2O_3, both of which absorb in the region). The data in Table 7 could not be used for absolute absorption

Table 7

RELATIVE EXTINCTION COEFFICIENTS FOR NO_2 AT 300.0°K

Wavelength (nm)	Io (nA)	I (nA)	Extinction Coefficient (cm^{-1} atm^{-1} @ 273°K, base e) (a)	(b)	Ratio
390.0	1.222	.635	16.35	16.13	1.014
391.0	1.269	.668	16.02	15.67	1.023
392	1.319	.672	16.84	16.26	1.014
393	1.370	.743	14.73	14.66	1.005
394	1.424	.778	15.09	14.90	1.013
395	1.480	.788	15.74	15.83	.994
396	1.539	.777	17.07	16.52	1.033
397	1.599	.879	14.94	15.23	.981
398	1.662	.834	17.22	17.22	1.000
399	1.727	.936	15.30	15.15	1.010
400	1.795	.867	18.17	18.17	1.000
401	1.864	.924	17.52	17.44	1.005
402	1.936	1.047	15.35	15.35	1.000
403	2.010	1.13	14.36	13.72	1.047
404	2.087	1.068	16.73	16.31	1.026
405	2.165	1.104	16.82	16.99	.990
406	2.246	1.230	15.04	14.49	1.038
407	2.329	1.383	13.01	12.76	1.020
408	2.415	1.254	16.36	16.03	1.021
409	2.502	1.251	16.71	15.86	1.054
410	2.592	1.377	15.79	15.52	1.017
411	2.684	1.437	15.60		
412	2.779	1.560	14.42		
413	2.875	1.350	18.88		
414	2.974	1.569	15.97		
415	3.075	1.605	16.24		
416	3.179	1.887	13.02		
417	3.284	1.854	14.28		
418	3.392	1.096	14.52		
419	3.502	1.948	14.19		
420	3.614	1.941	15.52		

(a) Calculated from data using 0.082 torr NO_2 plus helium to 21.7 torr, at 300.0°K with a path length of 398 cm.

(b) From Bass, Ledford, and Laufer (1976).

coefficients because of the uncertainty in $[NO_2]$ described earlier, using the "standard" mixture in which the NO_2 slowly varied.

At temperatures below room temperature, only Bass et al. (1976) have measured absorption coefficients at 235°K, between the temperatures of 225° and 247°K. The direct comparison is difficult because of the temperature differences, but agreement appears to be within experimental error. The precision of the low temperature data in Table 2 is much less at these temperatures because of the smaller signal levels. The mirror reflectivity increase from 390 to 420 nm caused the uncertainty in α to increase as the wavelength decreased. Thus, propagation of error analysis based on a 5% uncertainty to I/I_o at 420 nm leads to an uncertainty in α of ± 6%, while a 390 nm the values are ± 12% and ± 15%, respectively. These values are for 204°K. Other estimated uncertainties are also listed in Table 1.

The quantum yield data in Table 6 at room temperature are also in relatively good agreement with the lierature values of Jones and Bayes (1973) and Harker et al. (1977). At the short wavelengths, the agreement is better than at the longer wavelengths, although agreement is within the combined experimental error at all wavelengths. The data in Table 6 seem to indicate a slightly lower value for the quantum yields at longer wavelengths than the literature data. However, the agreement is certainly good enough to allow confidence in low temperature measurements taken in this study. The results in Table 6 at 223°C, while providing precise measurements of the NO_2 photolysis quantum yield, are not quite complete enough to reach final conclusions concerning the mechanism of NO_2 photodissociation. However, the following two observations may be made concerning the quantum yield wavelength dependencies at the two temperatures.

First, the reduction in quantum yield with reduced temperature was greater at long wavelengths than at short wavelengths. This occurs because 390 and 395 nm are below the dissociative cut-off wavelength, and thermal energy would not be necessary to dissociate the NO_2 at any temperature. Since the precision at the short wavelengths was limited by the low mirror reflectivities in this region, the small measured drop in quantum yield at short wavelengths is of limited significance, but would be very important in efforts to elucidate the NO_2 photolysis mechanism.

Second, performing the calculations to determine relative population as a function of rotational energy at a given temperature, using the symmetrical top approximation described in detail by Jones and Bayes (1973), and then comparing it with the data, one finds that the difference between the calculated and measured percentage reduction in quantum yields at a given wavelengths was within experimental error. The absolute measured value for the quantum yield at 223°K, however, was higher by 15% at 405 nm than the calculated value at the same temperature normalized to 0.78 at 397.8 nm. These two observations, coupled with the fact that the quantum yield is not unity at the thermal cut-off, tend to support previous speculations concerning a nondissociative, perhaps radiative, bound state that is stable above the dissociation limit of NO_2.

The data presented here, however, are not extensive or intensive enough to totally elucidate the detailed physical mechanism by which NO_2 photodissociates. The data were derived primarily to provide an accurate basis upon which to calculate stratospheric NO_2 photolysis rates in the absence of such an elucidation. Combination of the values for α and ϕ given in this report with the known photon fluxes and appropriate concentrations should yield values for stratospheric photolysis rates in the 390 to 420 nm region precise to within about 30% at 223°K, which is the worst case. Careful interpolation and extrapolation of the data in this report should yield the products $\alpha \cdot \phi_{NO}$ accurate to within about 25% for any temperature in the stratosphere from about 200° to 270°K.

CONCLUSIONS AND FUTURE WORK

The absolute absorption coefficient data developed on this project and elsewhere (Bass et al.; 1977, Johnston and Graham, 1974; Harker et al., 1977; Hall and Blacet, 1952; and Dixon, 1939) are in very good agreement at room temperature. The data at lower temperatures presented here for the first time seem to overlap well with the only other data at low temperatures, that of Bass et al. (1977). However, more temperatures were covered in this study, extending the lower temperature limit for such measurements down to 204°K. Interpolation and extrapolation of the data for any stratospheric temperature should thus be easily done for any specific wavelength to within 10%.

The quantum yield data provides values useful in calculating photolysis at 223°K to within about 15%. However, the data here and in the literature are not yet complete or precise enough to explain the mechanism of NO_2 photolysis that would allow functional quantitative correlations between the data at different temperatures.

Thus the following further studies should be undertaken to put the stratospheric NO_2 photolysis rates on a firm theoretical basis:

(1) More measurements are needed of quantum yields at other low temperatures.

(2) More wavelength interpolation is necessary to look for structure, especially at lower stratospheric temperatures.

(3) The recent studies by Bass et al.. (1977) and Harker et al. (1977) have indirectly indicated that there may be a temperature dependence of photolysis quantum yields at wavelengths shorter than the dissociation limit.

Thus since roughly 60% of the NO_2 present in the lower stratosphere is photolyzed in the wavelength region of 310 to 390 nm (calculation based on Leighton, 1962), the influence of temperature on NO_2 stratospheric photolysis rate in this wavelength region could be nearly equal to the effect on photolysis in the 390 to 420 nm region. Thus, the temperature behavior of the NO_2 photolysis quantum yield should be investigated in the region of 300 to 390 nm. Specifically, we suggest extending determination of NO_2 photolysis quantum yields at stratospheric temperatures to include this wavelength.

LITERATURE CITED

Bass, A. M., A. E. Ledford, and A. H. Laufer (1976), J. Res. Nat. Bur. Std., 80A, 143.

Bodenstein, M., and F. Boes (1922), Z. Physik. Chem. 100, 75.

Davis, D. S., J. T. Herron, and R. E. Huie (1973), "Absolute Rate Constants for the Reaction O (^{3}P) + NO_2 + O_2 Over the Temperature Range 230-339°K," J. Chem. Phys., 58, 530-535.

Dixon, J. J. (1939), J. Chem. Phys., 8, 157.

Hall, T. C., and F. E. Blacet (1952), J. Chem. Phys., 20, 1745.

Hampson, R. F., and D. Garvin (1973), "Chemical Kinetics Data Survey VI: Photochemical and Rate Data for Twelve Gas-Phase Reactions of Interest for Atmospheric Chemistry," NSB IR 73-207m, Physical Chemistry of Standards, Washington, D.C.

Harker, A. B., W. Ho, and J. J. Rato (1977), Chem. Phys. Lett. 50, 394.

Herzberg, G. (1966), Electronic Spectra of Polyatomic Molecules (Van Nostrand, New York, NY, p. 602.

Johnston, H. (1975), CIAP Monograph I, "The Natural Stratosphere of 1973," A. J. Grobecker, Ed. Final Report DOT-TSC-74-51, National Technical Information Service, Springfield, Virginia, 22151 (September 1975).

Johnston, H. S., and R. Graham (1974), Can. J. Chem., 52B, 1415.

Jones, I.T.N., and K. D. Bayes (1973), J. Chem. Phys., 59, 3119, and J. Chem. Phys., 59, 4837.

Kistiakowsky, G. B. (1930), J. Am. Chem. Soc. 52 (102).

Lee, E.K.C., and W. M. Uselman (1972), Disc Faraday Soc., 53, 125.

Leighton, P. A. (1962), Photochemistry of Air Pollution, Academic Press, New York, p. 29.

Pitts, J. M., J. H. Sharp, and S. I. Chan (1971), J. Chem. Phys., 42, 3655.

Stull, D. R., and H. Prophet (1971), JANAF Thermochemical Tables, 2nd Ed. Nat. Stand. Ref. Data Ser., Nat. Bur. Std. (U.S.), 37.

Uselman, W. M., and E.K.C. Lee (1973), J. Chem. Phys., 64, 3457.

Watanabe, K., M. Zelikoff, and E.C.Y. Inn (1953) AFCRC Technical Report No. 53-23, Geophysical Research Papers Number 21, "Absorption Coefficients of Several Atmospheric Gases," Geophysics Research Directorate, Air Force Cambridge Research Center, Cambridge, Mass.